

## Gated ion spectrometer for spectroscopy of neutral particles

S. Sharif,<sup>1</sup> J. Braenzel,<sup>2</sup> M. Schnürer,<sup>2</sup> R. Prasad,<sup>3</sup> M. Borghesi,<sup>4</sup> V. Tikhonchuk,<sup>5</sup> and S. Ter-Avetisyan<sup>6</sup>

<sup>1</sup>Department of Physics and Photon Science, GIST, Gwangju 500-712, South Korea

<sup>2</sup>Max Born Institute for Nonlinear Optics and Short Pulse Spectroscopy, Berlin 12489, Germany

<sup>3</sup>Institute for Laser and Plasma Physics, Heinrich Heine University, Düsseldorf 40225, Germany

<sup>4</sup>School of Mathematics and Physics, The Queen's University of Belfast, Belfast BT7-1NN, United Kingdom

<sup>5</sup>Centre Lasers Intenses et Applications, CEA, CNRS, University of Bordeaux, 33405 Talence, France

<sup>6</sup>ELI-ALPS, Szeged H-6720, Hungary

(Received 12 March 2017; accepted 21 July 2017; published online 8 August 2017)

A new design of an ion mass spectrometer for the laser-plasma particle diagnostic, which is capable to detect simultaneously also neutral particles, is described. The particles are detected with micro-channel-plate detector operating in a gated mode. This allows us to separate x-rays and energetic electrons from other stray plasma emissions, e.g., neutral particles, which hit the detector in the same place. The ion energies are measured with the spectrometer in energy intervals corresponding to their time-of-flight within the gating window. The latter also defines the energy interval of neutrals recorded with the same time-of-flight. The spectrum of neutral particles can be reconstructed by subsequently collecting different parts of the spectrum while applying different delays on the gate pulse. That *separation-in-time* technique (time-of-flight mass spectrometry) in combination with the *spatially separating* mass analyzer (ion mass spectrometer) is used for the neutral particles spectroscopy. Published by AIP Publishing. [<http://dx.doi.org/10.1063/1.4997192>]

### I. INTRODUCTION

Spectroscopy is a well-established diagnostic of charged particles emitted from laser-plasmas. The mass-spectrometer invented by Thomson in 1911<sup>1</sup> has been widely used for analyzing charged particles accelerated in laser plasmas. It provides a distribution of accelerated ions as a function of their energy, momentum, and mass-to-charge ratio. Several modifications have been introduced recently, which allow a more comprehensive analysis of plasma processes, in particular, the phenomenon of ion acceleration. The design of Thomson spectrometer employing the single particle sensitive micro-channel-plate (MCP) detector allowed a temporally<sup>2</sup> and spatially resolved<sup>3</sup> detection of accelerated ion distributions; simultaneous measurements of the ion and electron spectra along the same observation direction;<sup>4</sup> and precise measurements of the proton/ion trajectories<sup>5</sup> for proton deflectometry<sup>6</sup> and tomography<sup>7</sup> applications. Another important modification combines a Thomson spectrometer with an extreme ultraviolet (XUV) spectrometer.<sup>8</sup>

The generation of negative ions and neutral particles from a liquid spray target has been reported in Refs. 9–11. The charge exchange process, where energetic positive ions propagating through a cold liquid spray<sup>12</sup> capture one or two electrons, was found highly efficient. The interaction proceeds almost elastically, a fast ion that captures or loses an electron propagates essentially in the same direction as before the collision. This finding may have an impact in the further development of a new neutral atom and negative ion sources. Therefore, a precise characterization of these processes is highly important for the creation of a comprehensive and self-consistent model of negative ion and neutral particle beam generation. The major challenge for detection

is that all species, positive and negative ions and neutrals, should be characterised simultaneously and in the same direction.

In this letter, we are introducing a new method where a Time-of-Flight (TOF) analyzer for neutral particles is realized in a Thomson spectrometer. For that the MCP detector coupled to the phosphor screen is gated permitting to reveal the particle energy distribution due to their deflection in the magnetic field but also their temporal evolution according to the delay time between the plasma creation and gate pulse. This combination of TOF and Thomson spectrometers constitutes a detector for the ion and neutral particles spectroscopy.

### II. CONCEPT

Using a Thomson spectrometer, positive and negative ions are deflected in opposite directions in the magnetic and electric fields thus creating oppositely directed spectral traces at the detector screen, while undeflected neutral particles together with x-rays create a “zero point”—a bright central spot. Thus the trace of neutral particles is overlapped with the x-ray emission and there is no dispersion in energy.

The neutral particles are usually detected with a Time-of-Flight (TOF) mass-spectrometer. While a linear TOF system is rather simple, it has poor spatial and energy resolution compared to other mass analyzers. Another issue is interfacing a TOF spectrometer with an ion source emitting an almost continuous spectrum of various ion species as they are accelerated from the laser plasma.

Using a gated MCP detector in the Thomson spectrometer allows a temporal separation of emitted neutral particles from prompt x-ray photons that are hitting the same place

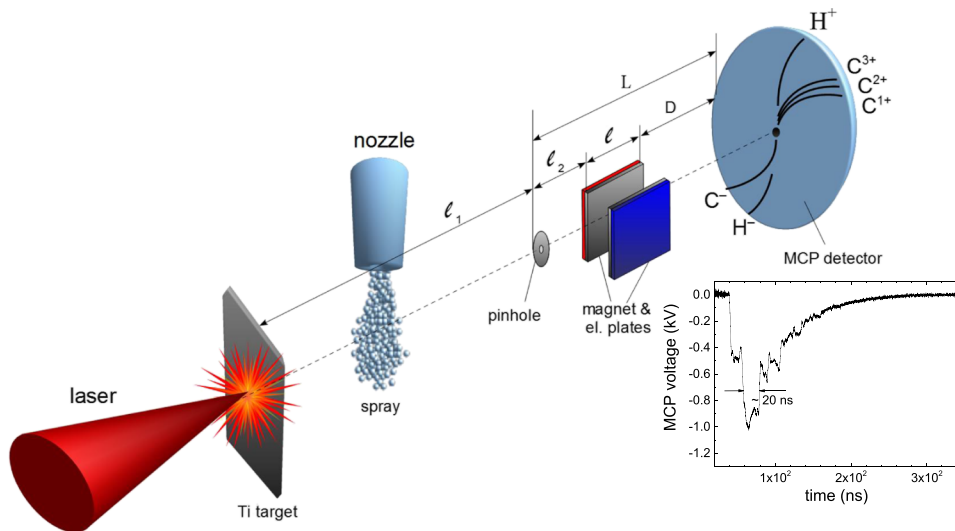


FIG. 1. Schematic of the experimental setup for measuring the fast positive and negative ions and neutral atoms when laser accelerated fast positive ions from the foil target propagate through a cold spray. The ion spectra and neutral atoms were measured simultaneously in a single laser shot using a gated MCP detector coupled to a phosphor screen. The image of the phosphor screen was taken with a cooled 12 bits Chroma CCD camera. In the inset is shown a typical gating pulse applied on a MCP plate.

of the screen. Moreover, spatially separated charge particles and neutrals having the same TOF are detected within the same gating time at the MCP. Therefore the velocity of all charged particles measured by their deflection inside the spectrometer is the same as the velocity of neutrals. The ion TOF can be calculated from their energies and masses measured in the spectrometer. This gives an advantage to estimate the energy of neutrals with the same accuracy as that of ions. Subsequently, by changing the gating time, one can reconstruct the energy distribution of charged and neutral particles simultaneously and make a direct comparison of their yields.

### III. SETUP AND METHOD

The negative ion and neutral atom beams were studied in a specific setup where the ion source and the spray target were separated.<sup>12</sup> The positive ions were accelerated in a foil target and propagated through a cold spray where negative ions and neutral atoms were formed via the electron capture and loss processes. The experimental scheme is presented in Fig. 1. The ions are accelerated from a 5  $\mu\text{m}$  Ti foil irradiated with 40 fs, 1 J Ti:sapphire laser pulses at an intensity of  $5 \times 10^{19}$  W/cm<sup>2</sup> under 45° of incidence. A directed ion beam formed through a  $d = (0.3 \text{ and } 1)$  mm pinhole placed at a distance of  $l_1 = 44$  cm from the source was analysed with a Thomson spectrometer with a magnetic field of 0.27 T and an electric field of 2-4 kV/cm both in a length of  $l = 5$  cm. The distance of the MCP from the source was  $l_1 + L = 79$  cm and  $D + l/2 = 9.5$  cm from the centre of magnet. A shot-to-shot fluctuation in ion emission from the Ti foil target was less than (1-2)% in numbers and energies at the similar irradiation conditions. Negative ions and neutral atoms were produced in a well characterised water spray<sup>13</sup> located at a distance of 4 cm from the foil. The spray was switched on or off<sup>12</sup> in order to compare the ion spectra with and without interaction with a spray.

An absolutely calibrated Thomson parabola spectrometer<sup>10</sup> was measuring the positive and negative ions in a single laser shot. The position of the particle on the spectral trace

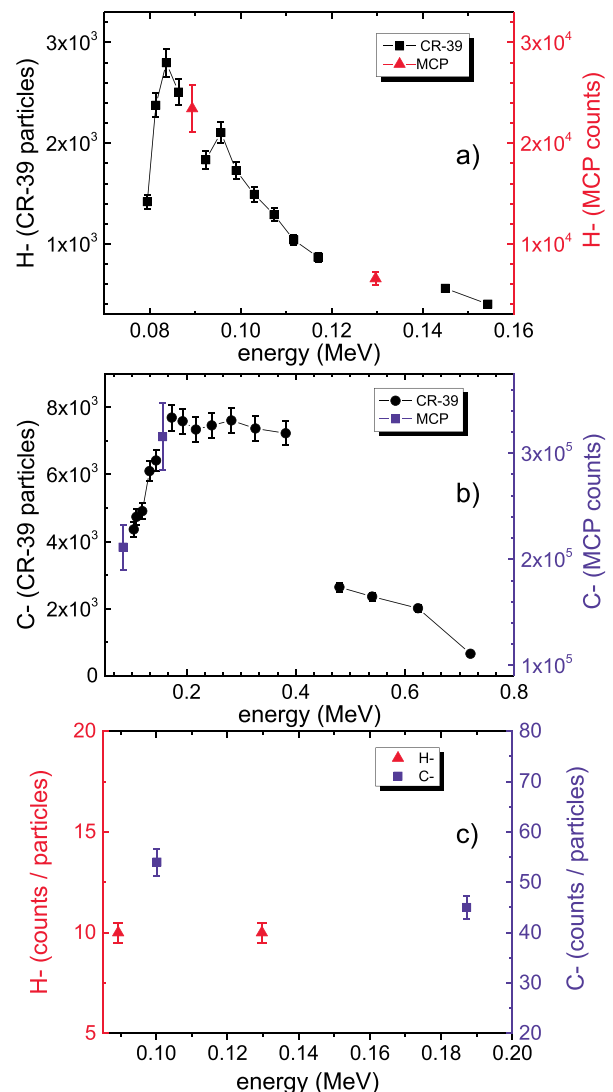


FIG. 2. Absolute number of (a) negative hydrogen (red) and (b) negative carbon (blue) ions counted on the stripes of slotted CR-39 plate (black) and corresponding counts on the CCD image of the MCP phosphor screen between the stripes. The data represent accumulated 25 consecutive shots. (c) The calibration analysis results for negative hydrogen and negative carbon ions.

depends on its energy: the higher is the ion energy, the less it is deviated from “zero point” where undeflected emissions, x-ray and neutral atoms, hit the detector.<sup>9</sup> To be able to measure also the energetic neutrals in the same setup and with the same detector, the MCP assembly (the MCP plate and the phosphor screen) was gated. The delay and the duration of the gate pulse were chosen according to the energy of particles and the energy interval of interest (from 20 ns up to 300 ns), respectively. A typical gate pulse applied to the MCP plate is shown in Fig. 1. Such a setup allowed us to take snapshots of ions and neutrals within the same velocity interval, which can be estimated from their TOF and also from the measured ion velocities in the Thomson spectrometer.

The detection system was calibrated by measuring a ratio between the count numbers of negative hydrogen ( $H^-$ ) and carbon ( $C^-$ ) ions at the charge-coupled device (CCD) image of the phosphor screen of MCP and the number of incident ions.<sup>10</sup> The MCP assembly response was also calibrated in a Thomson spectrometer for protons with energies up to 17 MeV and carbon ions up to 58 MeV in Ref. 14. This calibration for a quantitative data analysis as the MCP response depends on the energy and the species of the particles. Spatial precautions have been taken for stability of the amplitude of the gate pulse because its fluctuations can cause fluctuations of the MCP response to the particle impact. A timing stability of the duration and delay of the gated pulse was precisely deduced from the measurement of charged ion spectra by the spectrometer. However, the gate pulse was measured

with each measured spectra. In the experiments, we had fluctuation of the amplitude of the gate pulse within 10% where MCP gain is almost constant, and its duration and delay were fluctuating within the same order.

#### IV. MCP RESPONSE TO NEGATIVE IONS

A method of calibration of a Thomson–MCP assembly to the impact of negative hydrogen ( $H^-$ ) and carbon ( $C^-$ ) ions is similar to that used in Ref. 14. A slotted CR-39 track detector was placed in front of the MCP. The parabolic traces of the ions were partly detected on CR-39, while the ions passing through the gaps of a slotted CR-39 were detected on a MCP. A total number of 25 shots were accumulated on the CR-39 detector in order to reduce the statistical error, while the MCP was recording in a single shot mode. The tracks on CR-39 plates were recorder after etching in a 6N NaOH solution at a temperature of 70 °C in a water bath.

A number of particles on the CR-39 film in a given energy interval were correlated with a number of integrated counts on the CCD referring to the same energy interval and track. A response of the MCP to negative hydrogen and carbon ions was calculated by dividing the counts for a certain energy interval of the MCP image by the total particle numbers on the CR-39 plate in the same energy interval. The results shown in Fig. 2 demonstrate good agreement between the two detectors. The low particle number and a small pit size on the CR-39 in a

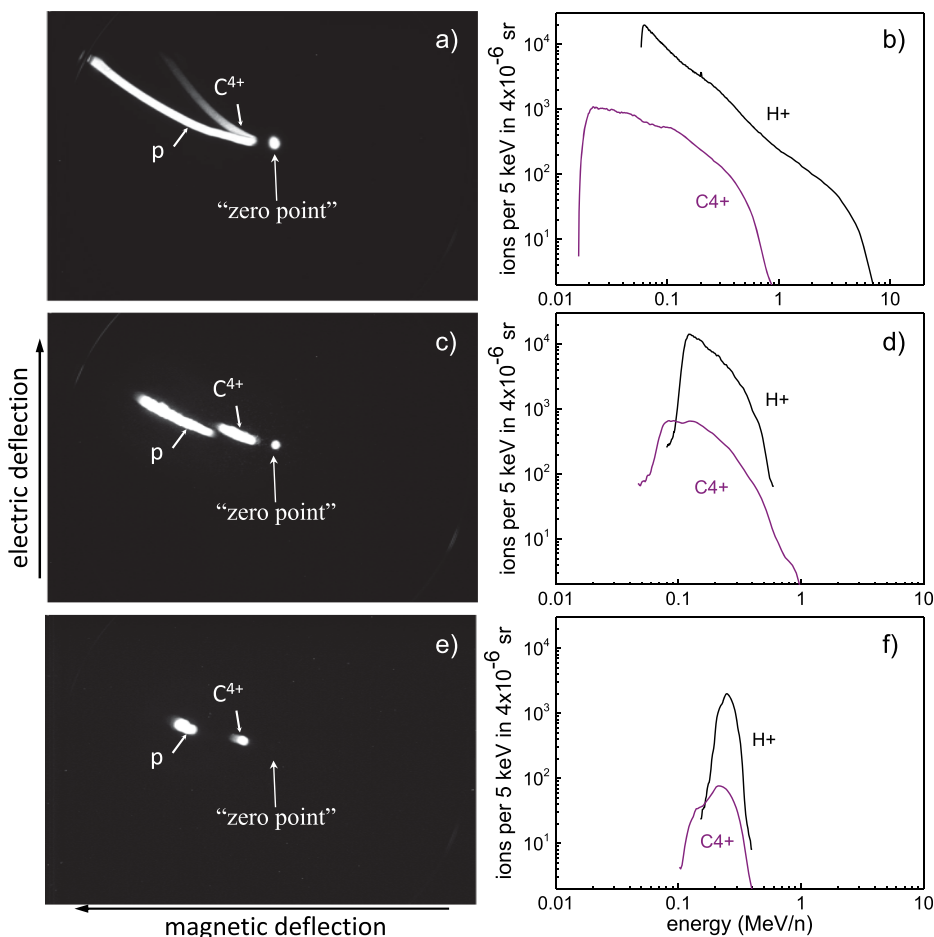


FIG. 3. CCD images of the ion spectra from the Ti foil target on a MCP screen (right column) together with energy distribution of ions (left column) deduced from these images when spray generator was switched off. [(a) and (b)] Without gating the MCP. The MCP was gated [(c) and (d)] with a delay of 90 ns for a time interval of 100 ns and [(e) and (f)] with a delay of 100 ns for a 60 ns time interval.

low energy range  $<0.08$  MeV result in a larger counting error (about 10%).

## V. MCP GATING

Creation of a well defined gate pulse applied to the MCP and the phosphor screen ( $-1$  and  $+4$  kV, respectively) is not a simple task. However, the actual gating time in our setup can be accurately defined by measuring the charged particle energy recorded with a Thomson spectrometer. Figure 3 (right column) shows CCD images of the ions accelerated from a Ti foil target on a MCP screen. Here we use the pinhole of a diameter  $d = 1$  mm and the spray generator was switched off. The ion energy distributions deduced from these images are shown in the left column. The upper row [panels (a) and (b)] shows the ions accelerated from the foil and no gating voltage was applied to a MCP. Only positive ions,  $H^+$  and  $C^{4+}$ , are present along with a strong “zero point” signal. The case of a MCP gated for a time interval of 100 ns with a delay of 90 ns is shown in Figs. 3(c) and 3(d). The bottom row, Figs. 3(e) and 3(f), corresponds to the gate time of 60 ns and a delay of 100 ns. An increase of the delay time from panels (c) to (e) only by 10 ns permitted to remove completely a signal at the “zero point,” which is mostly due to the x-ray emission from the target. Thus, the “zero point” detected at longer delays can be attributed to the neutral atoms.

Then a liquid spray generator was switched on (see Fig. 1) and the accelerated ions from a Ti foil passed through the spray. The results detected on the screen in that case are shown in Fig. 4. For the same gate pulse delay of 100 ns where the “zero point” was not detected in Fig. 3(e), a signal at the “zero point” is recorded in Fig. 4(a). It is due to the neutral carbon atoms ( $C^0$ ) generated in the spray<sup>9</sup> and arriving to the detector together with the other ions. The recorded energy interval for  $C^0$  is the same as the positive carbon ions as they have the same TOF.

A decrease of gating time leads to a reduction of the energy interval of the particles detected by the MCP. It is seen in Fig. 3 as shortening of the length of spectral traces. Further reduction of gating time will further reduce the length of spectral trace to the minimum size when it becomes a projection of the entrance pinhole. The ion spectra presented in Fig. 4 were measured through a 1 mm diameter pinhole with a MCP gating time of  $(20 \pm 2)$  ns delayed by 180 ns relative to the laser shot. The carbon ion traces in panel (a) have the size of the pinhole. There is no measurable dispersion in the carbon ion traces, while the protons are dispersed. This means that the spectral width of carbon ions is not resolved by our spectrometer. For singly ionized carbon ions, the expected spectral width is about 200 keV, if we take into account the imaging system with the uncertainty of about 5 pixels where 1 pixel is about  $100 \mu\text{m}$ . The different widths of the spectra of carbon ions in panel (b) are explained by a nonlinear dispersion of the spectrometer. Hence, a too short gating time in this example does not allow us to resolve the energy of carbon ions. This demonstrates a limit of the applied method, namely, the resolution of the spectrometer should be higher than the energy interval of the particles defined by gating time. As one can see, for the same gating time, the resolution

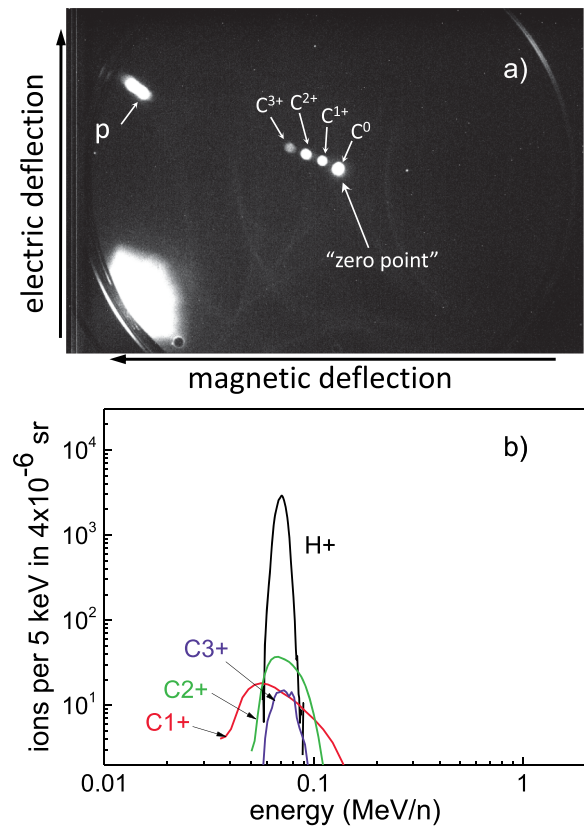


FIG. 4. CCD image of the ion spectra from the Ti foil target on a MCP screen (a) together with energy distribution of ions (b) deduced from this image when the spray generator was switched on. The ion spectra were measured with the MCP gating time of about  $(20 \pm 2)$  ns delayed by 180 ns relative to the laser shot.

of the spectrometer is sufficient for dispersing the recorded protons. The trace has a size bigger than the size of the pinhole.

The energy range of carbon  $C^{1+}$  ions to be detected at a delay time of 180 ns and a gating time of  $(20 \pm 2)$  ns is between 1.15 MeV and 0.93 MeV. This energy spread of 220 keV is almost the same as estimated from the measurements.

In the TOF of the particles from the relation  $v = L/t$ , the relative error in measuring the ion velocity would be

$$R_{TOF} = \frac{\Delta v}{v} = \frac{\Delta L}{L} + \frac{\Delta t}{t}. \quad (1)$$

The error of the measurement about 20% at the velocities  $v \approx 10^9$  cm/s ( $\sim 1$  MeV protons) can be achieved assuming the accuracy of measuring distance  $\Delta L \gtrsim 1$  mm and temporal resolution of the detector  $\Delta t \lesssim 0.2 L/v \approx 16 \times 10^{-9}$  s which is comparable to the applied gating time. This requirement of the detector can be reduced if the distance  $L$  is increased but could cause a reduction of density of the beam with given  $v$  at the detector plane by  $n_i \propto (L/r_0)^3$  which sets restrictions on  $L$  connected to the sensitivity of the detector.

For the Thomson spectrometer, the velocity of ions can be found from the electric ( $E$ ) and magnetic ( $B$ ) field deflections of the particles which in approximation of small deflection is described by

$$x = Ze \frac{E}{E_i} \frac{LD}{2}, \quad y = Ze \frac{B}{\sqrt{ME_i}} \frac{LD}{\sqrt{2}}, \quad (2)$$



where  $M = Am_p$ ,  $A$  is the mass number and  $m_p$  is the proton mass, and  $E_i$  is the ion energy.

From Eq. (2),  $v = E/B \cdot y/x$ , and the resolution of the Thomson spectrometer ( $R_{TS}$ ) can be expressed as<sup>15</sup>

$$R_{TS} = \frac{\Delta v}{v} = \frac{\Delta yx - y\Delta x}{yx} \leq \frac{(x+y)\delta}{yx}, \quad (3)$$

where  $\delta$  is a width of the parabola:  $\delta = dL/l_i$  (Fig. 1). In the experiments, the ratio  $L/l_i$  is approximately equal to unity and the resolution is defined mostly by the pinhole size  $d$ . For the energies about 1 MeV, the resolution of about 20% can be achieved with our geometry, including the pinhole size of 1 mm. Realistically the pinhole size can be taken as 0.1 mm and even smaller.

Thus, MCP gating allows us to take a snapshot of positive and negative ions and neutrals which are in the same velocity interval and separate them from a prompt x-ray flash from plasma. The particle energies are measured by their TOF and their spectral trace in the Thomson spectrometer. A resolution of a few percent at a given energy is easily achievable by changing the geometry and decreasing the pinhole size, which increases the accuracy of measurement of the particle energy.

## VI. RESULTS AND DISCUSSION

In order to increase the accuracy of ion energy measurements, a 0.3 mm entrance pinhole was used in the next

series of experiments. Typical CCD images of the MCP phosphor screen are shown in Fig. 5 (left column). The spectra of ions emitted from a Ti foil target are measured at constant voltages applied to the MCP assembly and without a spray.  $H^+$  and carbon ions from  $C^{1+}$  up to  $C^{5+}$  were recorded with the Thomson spectrometer where  $H^+$  and  $C^{4+}$  are dominating in terms of their flux. Then, the spray was switched on at about 200 ns after the laser pulse and the MCP was gated for 300 ns [Fig. 5(c)] and for 100 ns [Fig. 5(e)]. Three distinct new features were recorded: (i) appearance of negative ions and neutral particles at “zero point,” (ii) same spectral range for all ions, and (iii) no proton signal on the gated MCP.

Negative  $C^-$  ions are deflected in Fig. 5 in the direction opposite to positive ions and the neutrals are at a “zero point.” The x-rays were not detected due to the applied time delay. Appearance of negative ions and neutrals is connected to the propagation of positive ions accelerated from the foil through the spray. They are formed in interactions with cold particles as it is discussed in Ref. 12. Panels (c)–(f) in Fig. 5 show that the  $C^-$  and  $C^{1+}$  ions appeared at the same gating time, their spectral shapes are similar, and energies are also almost the same. Therefore, according to the charge exchange scenario,<sup>12</sup> the recorded neutrals at “zero point” should have the same energy as the positive and negative carbon ions. The measured signal in Figs. 5(c) and 5(e) at “zero point” consists mainly of neutral carbon atoms ( $C^0$ ). However, within the gating time, there could also be low energy (<40 keV)

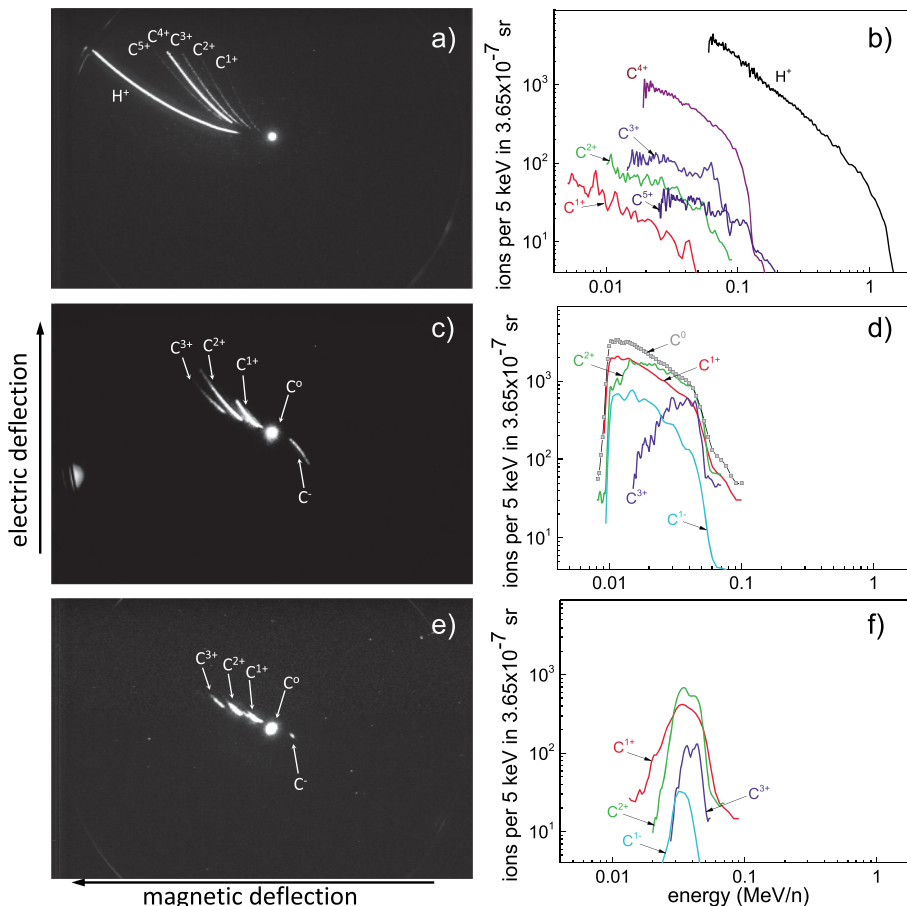


FIG. 5. CCD images of the ion spectra from the Ti foil target through a 0.3 mm entrance pinhole on a MCP screen (right column) together with energy distribution of ions (left column) deduced from these images. [(a) and (b)] The spray generator was switched off. [(c)–(f)] The spray was switched on at about 200 ns after the laser pulse. The MCP was gated [(c) and (d)] for 300 ns and [(e) and (f)] for 100 ns.

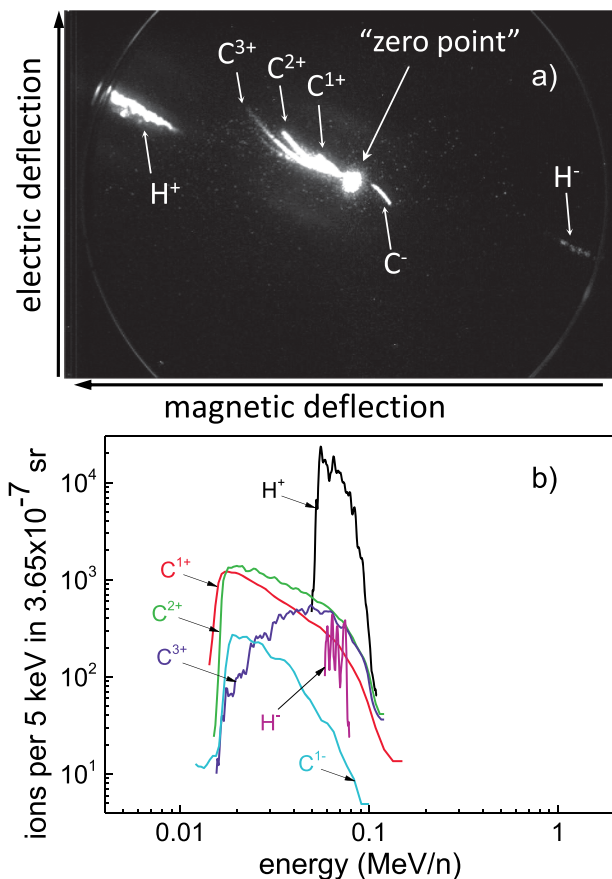


FIG. 6. CCD image of the ion spectra from the Ti foil target through a 0.3 mm entrance pinhole on a MCP screen (a) together with energy distribution of ions (b) deduced from this image when the spray generator was switched on for 300 ns and delayed by 180 ns relative to the laser shot. Low energy cut in hydrogen spectra is due to the detector edge.

neutral hydrogen atoms ( $H^0$ ) which is out of spectrometer detection range.<sup>10</sup> These two species will be contributing to the signal at “zero point.” Relying on the fact that the sensitivity of the detector for  $C^0$  is by a factor of four higher than for  $H^0$  (see Fig. 2), one can assume that the signal is generated mostly by  $C^0$ . By using the fact that the  $C^-$  and  $C^{1+}$  ions and  $C^0$  atoms are in equilibrium<sup>12</sup> and have been recorded in the same energy interval, their spectral shape should be similar. Using the MCP calibration data (Sec. IV), the spectrum of neutral carbon atoms ( $C^0$ ) can be simulated as shown in Fig. 5(d).

At the early gating time, where only  $H^+$  ions were detected, excluding the carbon ions, there was no signal at “zero” point, which suggests that  $H^0$  are not formed from high energy  $H^+$ . It is reasonable to think that  $H^0$  will be mostly formed at energies similar to  $H^-$  ions, which is at maximum 200 keV and low. Therefore, in this case, there will always be  $C^0$  with the same TOF as  $H^0$  particles and at “zero point” both neutrals will be detected. For instance, in Fig. 6, the hydrogen positive and negative ions can be seen on the detector screen when the gate pulse was delayed about 180 ns indicating that “zero point” consists of both neutral carbon and neutral hydrogen atoms but with the same energies. Their relative amount at “zero point” can be evaluated from the relative amount of detected corresponding positive and negative ions taking into

account the calibration of the detector (Fig. 2). By recording the ion species at different time delays, a full spectrum of neutrals can be reconstructed.

## VII. CONCLUSION

We have applied a gated MCP in a Thomson spectrometer for measurements of energy distribution of neutral particles. It is shown that the gating time defines the width of energy interval of recorded particles, and the delay between the particle acceleration and the gate pulse determines the recorded maximum energy. It is demonstrated that the neutral particles can be separated from the prompt x-ray flash of the plasma by applying an appropriate delay time. The spectrum of neutrals can be reconstructed by subsequently collecting different parts of the spectra controlled by the gate pulse delay. The method allows a significantly increase in the neutral particle energy resolution compared to the conventional TOF technique to the resolution limit of the Thomson spectrometer.

The capability of this diagnostic technique is not restricted by the phenomena discussed here. The temporally resolved ion and neutral particle spectra have a great potential for studying processes of acceleration of charged and neutral particles and measuring temporal characteristics of ion sources for different charge states and energies.

## ACKNOWLEDGMENTS

This work was performed under the ELI-ALPS Project (No. GINOP-2.3.6–15-2015–00001), which was supported by European Union and co-financed by the European Regional Development fund. This work was supported by Laser-Lab Europe Proposal No. MBI001886 and by the Deutsche Forschungsgemeinschaft (DFG) within the program Transregio 18. We thank F. Abicht for the support during the experiments.

- 1J. J. Thomson, “Rays of positive electricity,” *Philos. Mag.* **21**, 225 (1911).
- 2S. Ter-Avetisyan, M. Schnürer, and P. V. Nickles, *J. Phys. D: Appl. Phys.* **38**, 863 (2005).
- 3J. Schreiber, S. Ter-Avetisyan, E. Risse, M. P. Kalachnikov, P. V. Nickles, W. Sandner, U. Schramm, D. Habs, J. Witte, and M. Schnürer, *Phys. Plasmas* **13**, 033111 (2006).
- 4S. Ter-Avetisyan, M. Schnürer, S. Busch, E. Risse, P. V. Nickles, and W. Sandner, *Phys. Rev. Lett.* **93**, 155006 (2004).
- 5S. Ter-Avetisyan, M. Schnürer, P. V. Nickles, S. Sikollik, E. Risse, M. Kalashnikov, W. Sandner, and G. Priebe, *Rev. Sci. Instrum.* **79**, 033303 (2008).
- 6T. Sokollik, M. Schnürer, S. Ter-Avetisyan, P. V. Nickles, E. Risse, M. Kalashnikov, W. Sandner, G. Priebe, M. Amin, T. Toncian, O. Willi, and A. A. Andreev, *Appl. Phys. Lett.* **92**, 091503 (2008).
- 7S. Ter-Avetisyan, M. Schnürer, P. V. Nickles, W. Sandner, T. Nakamura, and K. Mima, *Phys. Plasmas* **16**, 043108 (2009).
- 8S. Ter-Avetisyan, B. Ramakrishna, D. Doria, G. Sarri, M. Zepf, M. Borghesi, L. Ehrentraut, H. Stiel, S. Steinke, G. Priebe, M. Schnürer, P. V. Nickles, and W. Sandner, *Rev. Sci. Instrum.* **80**, 103302 (2009).
- 9S. Ter-Avetisyan, B. Ramakrishna, M. Borghesi, D. Doria, M. Zepf, G. Sarri, L. Ehrentraut, A. Andreev, P. V. Nickles, S. Steinke, W. Sandner, M. Schnürer, and V. Tikhonchuk, *Appl. Phys. Lett.* **99**, 051501 (2011).
- 10R. Prasad, F. Abicht, M. Borghesi, J. Braenzel, P. V. Nickles, G. Priebe, M. Schnürer, and S. Ter-Avetisyan, *Rev. Sci. Instrum.* **84**, 053302 (2013).
- 11R. Rajeev, T. M. Trivikram, K. P. M. Rishad, V. Narayanan, E. Krishnakumar, and M. Krishnamurthy, *Nat. Phys.* **9**, 185 (2013).

- <sup>12</sup>M. Schnürer, F. Abicht, R. Prasad, M. Borghesi, G. Priebe, J. Braenzel, A. Andreev, P. V. Nickles, S. Jequier, V. Tikhonchuk, and S. Ter-Avetisyan, *Phys. Plasmas* **20**, 113105 (2013).
- <sup>13</sup>S. Ter-Avetisyan, M. Schnürer, H. Stiel, and P. V. Nickles, *J. Phys. D: Appl. Phys.* **36**, 2421 (2003).
- <sup>14</sup>T. W. Jeong, P. K. Singh, C. Scullion, H. Ahmed, K. F. Kakolee, P. Hadjisolomou, A. Alejo, S. Kar, M. Borghesi, and S. Ter-Avetisyan, *Rev. Sci. Instrum.* **87**, 083301 (2016).
- <sup>15</sup>S. Sakabe, T. Mochizuki, T. Yamanaka, and C. Yamanaka, *Rev. Sci. Instrum.* **51**, 1314 (1980).